JOURNAL OF ENERGY SYSTEMS

2025, *9*(1)

2602-2052

DOI: 10.30521/jes.1523522

Research Article

Energy management technique of hybrid energy storage system-based DC microgrid

Mohammed Abdulelah Albasheri*
University of Médéa, Department of Technology, Laboratoire de Recherche en Electrotechnique et Automatique, Médéa, Algeria,
albasheri.mohamed@univ-medea.dz
Ouahid Bouchhida
University of Médéa, Department of Technology, Laboratoire de Recherche en Electrotechnique et Automatique, Médéa, Algeria,
bouahid2000@yahoo.fr
Youcef Soufi
University Echahid Larbi, Departement of Electrical Engineering, Laboratoire du génie Electrique-Labget, Tébessa, Algeria,
y_soufi@yahoo.fr
Abderrezzak Cherifi
IUT de Mantes-en-Yvelines, Laboratoire END-ICAP - UMR 1179, Université Paris Saclay-Versailles, France,
abderrezzak.cherifi@uvsq.fr
Mujammal Ahmed Hasan Mujammal
University of Médéa, Department of Technology, Laboratoire de Recherche en Electrotechnique et Automatique, Médéa, Algeria,
mujammalidole@gmail.com
Abdelhafidh Moualdia
University of Médéa, Department of Technology, Laboratoire de Recherche en Electrotechnique et Automatique, Médéa, Algeria,
amoualdia@gmail.com

Submitted: 29.07.2024
Accepted: 06.02.2025
Published: 31.03.2025

* *Corresponding Author*

Abstract: The generation of variable energy from photovoltaic (PV) is significantly affected by unpredictable fluctuations due to weather changes. Additionally, the variability in load demand is a critical consideration for microgrid. Consequently, the implementation of an energy storage system is essential to address these challenges. This study presents a novel energy management technique (EMT) for hybrid energy storage systems (HESS). The innovative approach incorporates a low-pass filter (LPF) to optimize power distribution between batteries and supercapacitors (SC), thereby enhancing system stability and prolonging battery life. The proposed LPF-based EMT facilitates optimal power allocation, improves system stability by effectively filtering high-frequency power fluctuations, and extends battery life through reduced stress and optimized charge-discharge cycles. It developed a comprehensive system model to enable accurate simulation and analysis, supported by rigorous experimental validation that demonstrates the effectiveness of our method. This approach successfully redirects high-frequency power demands to the SC, stabilizing the DC link voltage. Comprehensive simulations indicate the system's capability, revealing quantitative improvements in battery performance and efficiency across various LPF time constants τ, representing a significant advancement in renewable energy control. The simulation results confirm that the proposed architecture and system representation achieve optimal DC link voltage stability. Furthermore, increasing the τ reduces the state of charge (SOC) of the battery, contributing to an overall increase in battery lifespan.

Keywords: *Battery, DC microgrid, Energy management, Photovoltaic (PV), Supercapacitor*

Cite this paper as: Albasheri MA, Bouchhida O, Soufi Y, Cherifi A, Mujammal MAH, & Moualdia A., Energy management technique of hybrid energy storage system-based DC microgrid. *Journal of Energy Systems 2025; 9*(1): 36-51, DOI: 10.30521/jes.1523522

2025 Published by peer-reviewed open access scientific journal, JES at DergiPark (https://dergipark.org.tr/jes)

Nomenclature	Descriptions	Nomenclature	Descriptions
EMT	Energy management technique	MG	Microgrid
PMS	Power management strategy	DCMG	Direct current microgrid
RES	Renewable energy source	SOC	State of charge
PV	Photovoltaic	LPF	Low pass filter
HESS	Hybrid energy storage system	τ	Time constant of low pass filter
HES	High energy storage	MPPT	Maximum power point tracking
HPS	High power storage	PI	Proportional-Integral
HF	High frequency	PWM	Pulse width modulation
LF	Low frequency	P&O	Perturb and observe
SC	Supercapacitor		

1. INTRODUCTION

The contemporary power system increasingly prioritizes the integration of environmentally friendly technologies, driven by the dual imperatives of energy conservation and the rapid incorporation of renewable energy sources. Currently, wind farms and PV systems are the predominant technologies in this arena. Among these, PV technology stands out due to its favorable characteristics, including affordability, high efficiency, minimal maintenance requirements, and reliable performance. However, the viability and energy production of PV is significantly influenced by variable external conditions such as temperature, irradiance, partial shading, and humidity. These fluctuations can adversely affect the stability of the connected system [1-2]. Among renewable energy sources, solar power is considered the most significant owing to its limited distribution in off-grid regions. This kind of technology is not only economically efficient nevertheless well-developed and straightforward to implement [3]. Solar power is particularly vital in off-grid regions, where its limited distribution makes it a crucial resource. While PV technology is economically advantageous and relatively straightforward to implement, the intermittent nature of sunlight leads to substantial variations in power output. Consequently, there is a pressing need to design an effective energy storage system that can manage these power fluctuations and accommodate changes in consumer demand.

In standalone solar power systems, an irregular charging pattern combined with battery storage can reduce battery lifespan. Although batteries offer significant energy density, they are characterized by lower power density, slower dynamic response, and limited charge/discharge rates [4,5]. In contrast, SC possess high power density but limited energy capacity. The integration of batteries and SC in HESS capitalizes on their complementary attributes, leading to reduced battery size and enhanced longevity [6,7]. The dual use of batteries and SC has proven effective in various applications, including microgrids [8,9], electric automobile [10], uninterrupted electricity supply [11,12], and wind energy [13].

The architectures and management strategies of battery-SC systems have been extensively reviewed in the literature [14,15]. Reports indicate that optimization-based approaches yield the most efficient power distribution between batteries and SC, thereby improving overall system efficiency. HESS typically consists of high-energy storage (HES) and high-power storage (HPS), which collectively mitigate low and high-frequency power fluctuations within microgrids (MG) [16]. Various combinations of HESS are employed in MG, including battery-SC configurations, pumped hydropower storage-battery systems [17], compressed air energy storage flywheel energy storage (CAES-FES), fuel cell-hydrogen, and battery-thermal energy storage (Battery-TES). The most commonly utilized configuration involves a combination of batteries and SC, which effectively addresses significant power fluctuations while regulating the SOC levels to enhance battery longevity.

Recent studies, such as [3], have provided comprehensive examinations of battery and SC HESS for standalone PV systems in rural electricity applications. Most research has focused on the coupling of battery-SC HESS with solar or wind resources for off-grid operations [18]. These studies often address continuous power load scenarios within a DC microgrid framework, employing decentralized control strategies that manage HESS parameters without external communication considerations. EMT have been widely explored in numerous studies [19,20]. For instance, [21] presents a rule-based fuzzy logic power management technique (FL-PMT) designed for autonomous PV systems with HESS. Additionally, a centralized control and energy management system (CAEMS) has been introduced in [22,23], which efficiently manages energy distribution between the power grid, loads, and generating sources. However, electrical quality issues are often overlooked in these approaches. The primary challenge remains the development of an effective EMT. Various methods for managing energy within HESS have been considered to enhance the electrical efficiency of HPS [24,25]. EMT can be categorized into three main groups: optimization-based methods [26,27], rule-based techniques [28], and, more recently, learning-based approaches.

The algorithms controlling power flow and interconnections among various storage units in hybrid systems are pivotal for effective power sharing. This can be addressed through HESS that combine both active and passive parallel configurations [15]. Table 1 highlights the comparisons between the researched studies and the proposed study.

Table 1. Summary of related work in the literature.

Ref.	Description	Disadvantages
[29]	Propose a smoothing controller using fuzzy logic that adjusts the filtering τ according to the current solar power ramp rate to prevent battery overexertion.	A hybrid storage system that facilitates energy distribution based on frequency was not used.
[30]	The Filter-Based Method (FBM) is used for energy management in HESS, which include batteries and SC, to avert early deterioration of storage devices due to deep discharge.	More complexity in implementation and verification of stability and increased use of the battery. Supplementary techniques for the calibration of the included loops
[31]	Present the RMS current gain in batteries, the rise in energy losses, the overall energy efficiency, and the surge load power elimination rate.	The energy loss resulting from sluggish battery reaction is disregarded, impacting the system's stability.
[32]	Suggested the allocation of energy between batteries and SC, using a low-pass filter to mitigate peak current on batteries and redirect it to supercapacitors.	DC voltage exhibits instability with significant fluctuations throughout the transition of energy generation and consumption.
[33]	A hierarchical adaptive energy management system for hydrogen fuel cell hybrid train power systems is developed, integrating frequency decoupling with data-driven deep deterministic policy gradient (DDPG) methods.	The complexity of reinforcement learning-based EMS to consider multiple time steps.
[34]	An energy management strategy (EMS) for fuel cell hybrid electric vehicles (FCHEV) based on frequency decoupling using a fuzzy control mechanism.	The method failed to create a balance in energy distribution due to the complex fuzzy logic design.
[35]	A control technique for automated load shedding and power management in a microgrid using photovoltaic systems, DFIG-based wind energy, diesel generators, and local loads.	There is no storage system to reduce the stress on the battery and the control method is more complex and difficult to implement.
Proposed work	Energy management-based decoupling frequency for microgrid includes PV with battery and SC evaluated with various τ.	Simplest implementation and more stability. SC delivers high-frequency current components for longer durations and reduces battery deterioration compared to prior cases.

This work proposes the development of a solar energy system that incorporates a HESS consisting of batteries and SC. An innovative EMT is introduced, focusing on the allocation of energy between these two distinct storage devices. A novel approach is proposed to include an additional factor in the design of a proportional-integral (PI) controller, aimed at ensuring the stability of DC bus voltage and regulating the operation of the bidirectional converters connected to the batteries and SC. The DC link voltage is maintained at a stable reference level of 100 V. In addition, two PI controllers are employed to compute the reference current for both batteries and SC. The energy allocation between batteries and SC is determined using LPF, which effectively removes high peak currents from the batteries and directs them toward the SC. The filter constant regulates the energy consumption by both storage elements.

The article presents the following significant contributions:

Provide a review of the various architectures used to connect SC and batteries to the DC bus voltage and load. This comparison highlights the advantages and disadvantages of each architecture.

A novel technique for regulating the DC link voltage and the bidirectional converters through current control is proposed. The advantage of this innovative approach is that it stabilizes the DC bus voltage under varying τ values of the LPF.

EMT is suggested for the allocation of energy between the batteries and SC.

This paper is organized as follows. In Sec. 2, the configuration of the system proposed. The EMT is explained in Sec. 3. In Sec. 4, the results and discussion from the simulation process is presented. Finally, the concluding remarks are given in Sec. 5.

2. SYSTEM CONFIGURATION

The DC microgrid system is comprised of PV source, storage in the form of batteries, SC, and DC load, as seen in Fig. 1. PV source is the primary source of power and is employed the maximum power point tracking (MPPT) to produce as much energy as possible. DC/DC boost converter link it to a common dc link. HESS is connected to a DC link through a DC/DC bidirectional converter for each storage devices. HESS is used to adjust the DC voltage V_{DC} at the DC link, DC load is connected directly to the link voltage without converter.

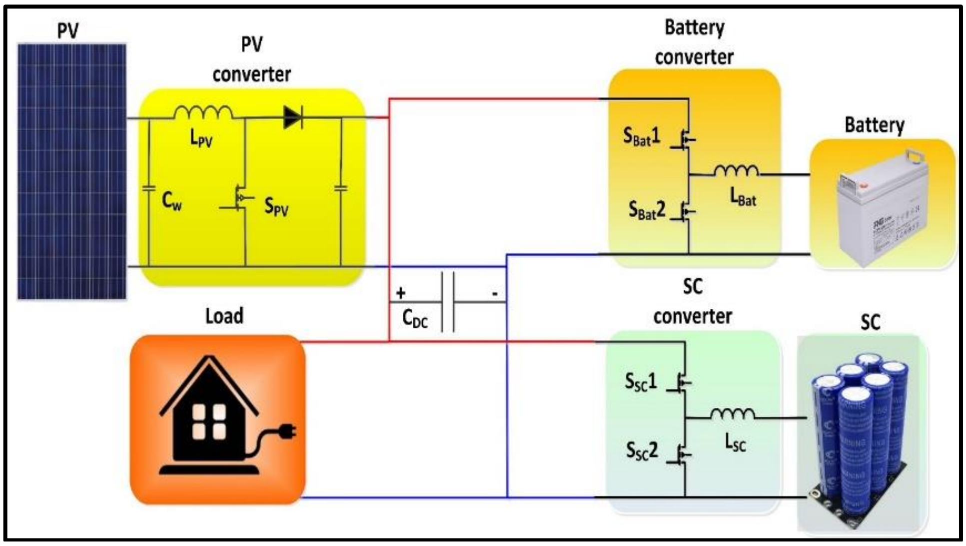

Figure 1. DC microgrid structure

2.1. Model of PV System

Different mathematical models of solar energy were developed to introduce their characteristics and behavior caused by the physical construction of PV cells. In this work PV model comes from [29,30]. PV voltage-current characteristics may be summarized as follows equation:

$$I_{pv} = I_{ph} - I_0 \left[exp\left(\frac{q(V_{pv} + R_s \cdot I_{pv})}{AN_s KT_j} \right) - 1 \right] - \frac{V_{pv} + R_s \cdot I_{pv}}{R_{sh}} \tag{1}$$

MPPT approach must be used to manage solar systems in order to obtain the maximum power generated from PV panels, Fig. 2 depicts a diagram of a novel control scheme that can conduct MPPT on a PV system equipped with a boost converter [36], the outer loop reference voltage v_{pv} can be generated using any voltage-based MPPT technique. The MPPT algorithm requires current $i_{pv}$and voltage v_{pv} measuring from PV systems (e.g., P&O) [37,38].

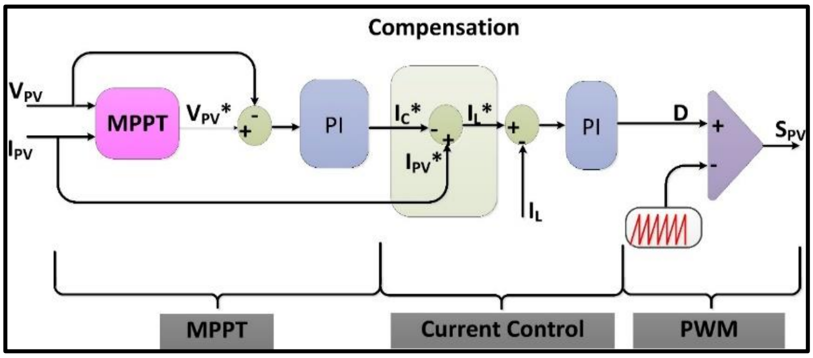

Figure 2. block diagram of MPPT

2.2. Battery Storage System Modeling

Using a battery and SC mix may be beneficial for renewable energy systems since it can support a broad range of energy and power consumption, especially solar power systems. It is feasible that new permutations might emerge. Here are some examples of how a (HESS) is often configured [39].

The batteries and SC are directly connected to the demand load in the passive parallel hybrid design. The SC's immediate link operates as a LPF. Since no special control mechanisms are required, it may be implemented quickly and easily. because of the way it was built. In addition, the balance power and energy between the battery storage and SC is unregulated, meaning that it is solely affected by parasitic elements. Furthermore, the voltage of the DC connection fluctuates depends on the amount of voltage produced by the battery, which has an effect on the design of the load. a graphic that illustrates the many configurations that may be used for HESS. Because of its capabilities, a bidirectional buck-boost converter enables a larger range of applications for the SC's voltage. In this design, there is just one changeable power source. To control the power of the SC, the bidirectional converter must be larger. Furthermore, the nominal voltage of the SC storage might be reduced. Because the battery is directly linked to the DC connection, changing the voltage there is difficult [40].

Depending on the configuration of the SC and battery, the voltage of battery may be maintained higher or lower than the SC voltage. The SC acts as LPF between the DC connection and the rest of the system. The system design for this topology may change the DC connection voltage to maximize SC energy utilization, but this has no effect on the battery's capacity [41]. Because it is able to withstand a wide variety of voltage changes, the capacitor may be used to the maximum degree possible. Both the SC and the battery power in this system have the potential to be managed independently, provided that their supply conditions and charge states are taken into account. This design's primary drawback is that it calls for a greater number of individual components, which drives up the overall price [42].

2.3. Classification of Energy Storage

HESS is connected to MG and uses several converter architectures that have a significant impact on system performance, operation, and prices. Fig. 3. shows three types of converter architectures used for combining HPS and HES for HESS: Passive, semi-active, and fully active. The total number and position of DC-DC converters that allow two directions power flows between storage devices, and load are the most significant distinctions between these architectures.

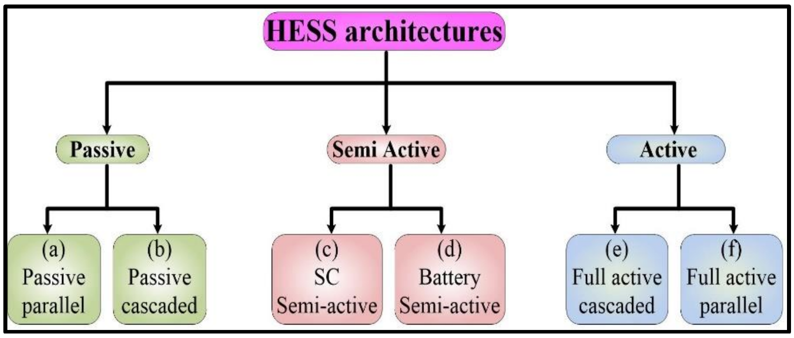

Figure 3. HESS classification

In the passive structure, high power storage and high energy storage terminals are directly connected to the DC link Figs. 4(a,b), Power-sharing in MG is determined by the electrical properties and time constant of the HESS element. Due to the significant differences in voltages between high power storage and high energy storage , the HPS abilities cannot be fully employed, resulting in limited flexibility and poor volumetric efficiency. During vicissitude, the passive-HESS architecture is subject to cascaded failure owing to the DC link. Battery-SC HESS architecture, the voltage of SC should be larger than a DC link and the voltage of battery, SC cannot use the absolute limit, which reduces SC efficiency [43].

This is the original notion of HESS topology and is seldom used in real-world utilization [44]. Semi active architectures are of two types: either a DC/DC converter coupled to one of the storage devices and other linked directly, as illustrated in Figs. 4(c,d), The semi-active topology allows for partial control flexibility.

- HES semi active architecture: When the DC/DC converter is coupled to the battery in battery-SC HESS, the current of battery rejects transients; nevertheless, the load voltage regulation responsibility restricts the SC's operational voltage range. The direct connection of the SC causes the voltage on the DC bus to vary. To stabilize DC link voltage, a big capacity of SC must be used, which raises costs [45].

- HPS semi-active architecture: When SC is linked via DC-DC converter, SC may function over a wide range of voltage; nevertheless, load transients may still impact the battery current [3]. The direct connection of the battery will ensure that the DC bus voltage remains steady. However, the chosen converter must tolerate significant voltage variations and strong current transients, which raises costs [46]. The semi-active topology allows for partial control flexibility. This architecture is only used in situations when there is little need for control and a considerable budgetary restriction.

The active architecture includes separate bidirectional DC-DC converters for each energy storage device to control, as illustrated in Figs. 4(e,f), The fundamental advantage of an active architecture is that the power of each ESS may be actively controlled. However, the disadvantage is that it increases system complexity, creates losses, and raises cost. Active architectures are divided into three types: cascaded, parallel, and multiple input. In Ref. [47], presented a parallel active architecture for battery-SC, which linked to the DC bus independently via separated DC-DC converters and subsequently fed power to the grid. This architecture enhances conversion efficiency and shortens power processing steps. Parallel active architecture is often utilized for microgrid.

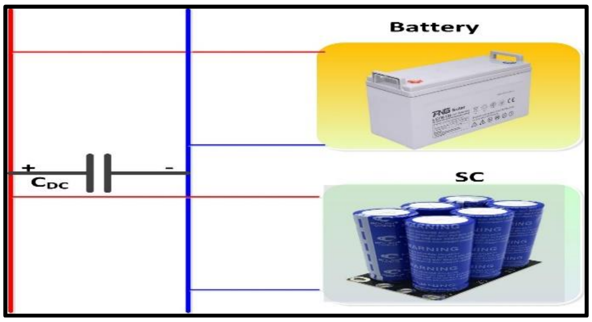

(a) Passive parallel

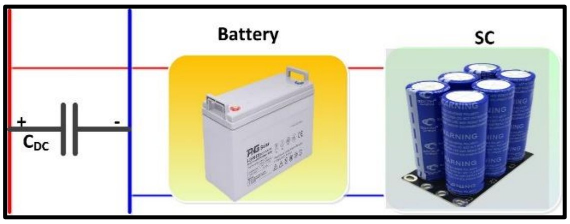

(b) Passive cascaded

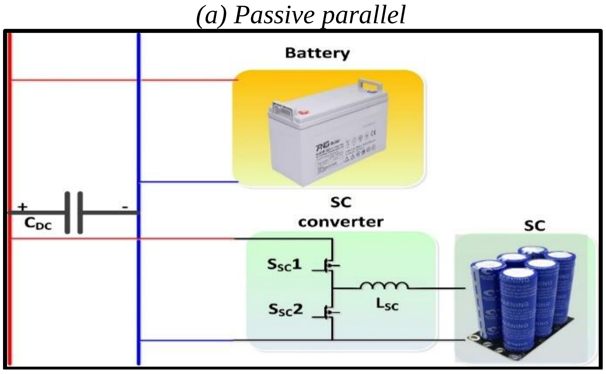

(c) SC semi-active

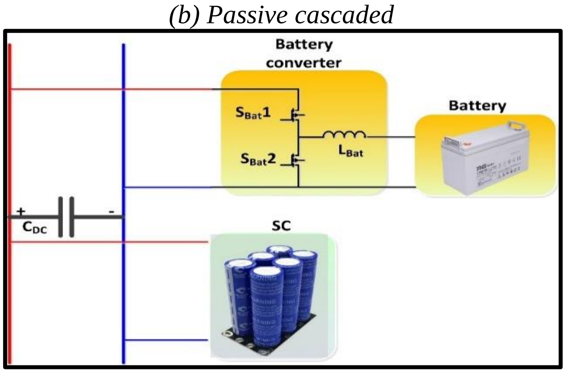

(d) Battery semi-active

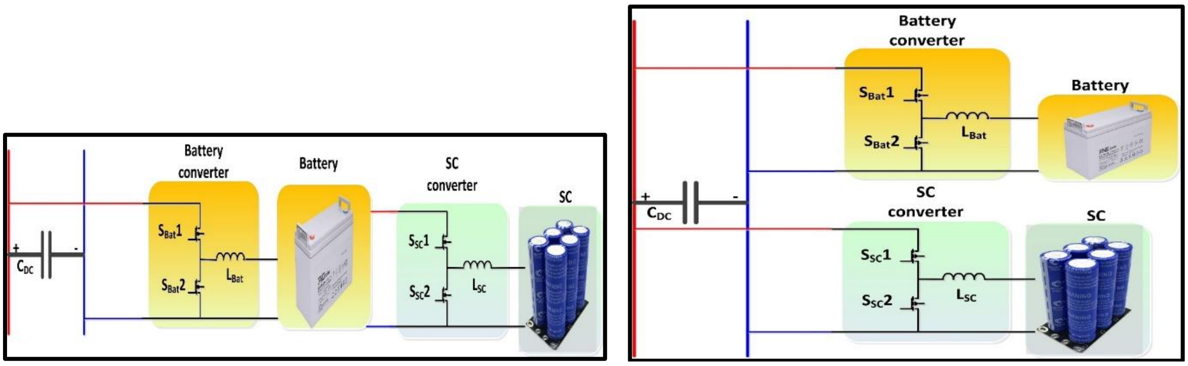

(e) Full active cascaded *(f) Full active*

Figure 4. HESS architectures

The parallel active topology is broadly employed in MG. The active topology has several advantages as follows [48]:

1) Separated control of HESS units offers extra flexibility,
2) Various control strategies can be employed,
3) The system voltage is independent of the voltage levels of ESS units,
4) It enhances the intrinsic fault tolerance capacity,

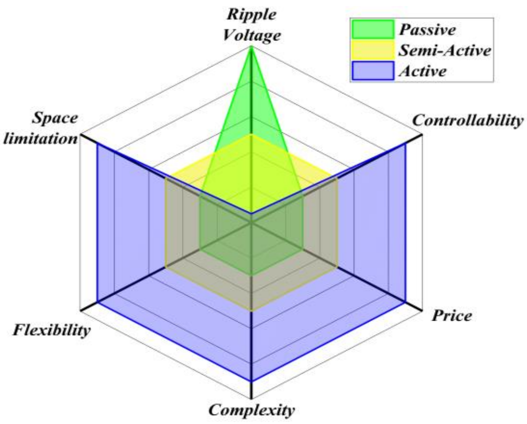

Figure 5. Comparative of indicators for HESS designs

Various indicators of HESS topologies are shown in Fig. 5. The active design offers superior flexibility, controllability, and voltage stability; however, it is accompanied by higher costs compared to alternative topologies. Additionally, it has more space limits.

3. ENERGY MAMAGEMENT STRATEGY

Fig. 6 depicts a block diagram that visually represents the suggested control approach. This technology enhanced the longevity of the battery by reducing the strain associated with its charging and discharging procedures. Throughout the examination, the state of charge of the energy storage systems has been found to be within acceptable boundaries. The PI controller computes the total current demand ($I_{tot}*$) by evaluating the error via comparing the average voltage of DC link (V_{dc}) with the desired voltage reference ($V_{dc}*$). The high and low frequencies of the total current ($I_{tot}*$) are represented by the terms ($I_{\mathrm{LFC}}*$) and ($I_{\mathrm{HFC}}*$) accordingly. The following phrases provide an explanation for the low-frequency elements.

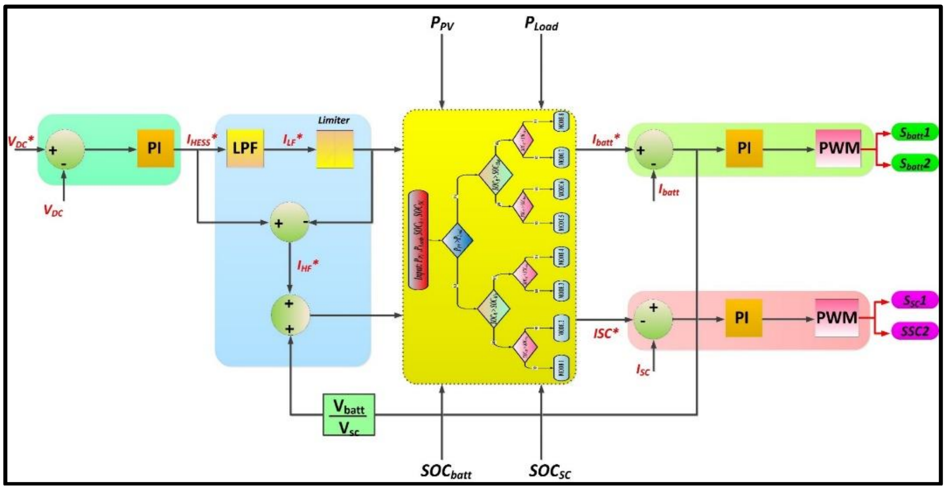

Figure 6. Suggested EMT scheme.

$$I_{LFC} *= f_{LPF}(I_{tot} *) \tag{2}$$

The function used for the LPF in this technique is $f_{LPF}(I_{tot} *)$. A rate limiter is a component with a low frequency that controls the rates at which the battery charges and discharges. Consequently, the battery is supplied with a consistent reference current [49].

$$I_B *= f_{RL}(I_{LFC} *) \tag{3}$$

where the function of rate limit is f_{RL} (.). whole time (I_B) compared with the current obtained from battery $(I_B *)$, the error between $(I_B *)$ with (I_B) is send to the PI control. The PI controller generated the duty ratio d_B and delivered it to the generator's (PWM), which generates pulses for the battery switches (S_{B1}andS_{B2}). The high frequency component $I_{HFC} *$ is expressed as;

$$(I_{HFC} *). = I_{tot} * -I_B * \tag{4}$$

Because of its sluggish dynamics, the battery may not be capable of keeping pace with the $I_B *$ right method. As a result, the compensator was used [50].

$$P_{B\_uncomp} = \left(I_{HFC} * + I_{B\_err}\right) * V_B \tag{5}$$

Where the battery voltage V_B and SC voltage $V_{SC}$are placed for mitigate the uncompensated battery current. Hence, SC's reference current $(I_{SC} *)$ is identified as [51];

$$I_{SC} *= \frac{P_{B\_uncomp}}{V_{SC}} = \left(I_{HFC} * + I_{B\_err}\right) * \frac{V_B}{V_{SC}} \tag{6}$$

The term(V_{SC}) is voltage of SC, and reference current of SC is $(I_{SC} *)$ and the actual SC current (I_{SC}) are contrasted for measure the error. The PI controller produces the duty ratio d_{SC} so that the generator PWM may supply switching pulses that are compatible with the SC switches (D_{SC1} and D_{SC2}). By using the formulas provided above, one can derive the following formula:

$$C_{DC}\frac{dV_{DC}}{dt} = i_{L_{SC}}\frac{V_{SC}}{V_{DC}} - \frac{V_{DC}}{R_L} - I_{DC} \tag{7}$$

the representation of the transfer function of DC link voltage is developed as follows;

$$FTx(s) = \frac{V_{DC(s)}}{I_{DC}(s)} = \frac{V_{SC}R_L}{\frac{R_L C_{SC}}{2}s + 1} \tag{8}$$

The equation presented the transfer function of the PI controller.

$$C_{dc}(s) = K_{p_{DC}} + \frac{K_{i_{DC}}}{s} \tag{9}$$

resulting in:

$$FTBF\ (s) = \frac{K_{P_{DC}}R_L V_{SC}\left(s + \frac{K_{i_{DC}}}{K_{P_{DC}}}\right)}{K_{p_{DC}}R_L V_{SC}\left(s + \frac{K_{i_{DC}}}{K_{p_{DC}}}\right) + s\left(\frac{R_L C_{SC}}{2}s + 1\right)} \tag{10}$$

resulting in:

$$FTBF(s) = \frac{K_{p_{DC}}R_L V_{SC}\left(s + \frac{K_{i_{DC}}}{K_{p_{DC}}}\right)}{\frac{R_L C_{SC}}{2}s^2 + \left(K_{p_{DC}}R_L V_{SC} + 1\right)s + K_{p_{DC}}R_L V_{SC}\frac{K_{i_{DC}}}{K_{p_{DC}}}} \tag{11}$$

By comparing the denominator with the equivalent of the canonical form, we obtain,

$$\begin{cases} K_{i_{DC}} = \dfrac{\omega_n^2 C_{SC}}{2V_{SC}}, & \omega_n^2 = \dfrac{2}{C_{SC}}V_{SC}K_{i_{DC}} \\ K_{p_{DC}} = \dfrac{\xi\omega_n R_L C_{SC} - 1}{R_L V_{SC}}, & 2\xi\omega_n = \dfrac{2}{R_L C_{SC}}\left(K_{p_{DC}}R_L V_{SC} + 1\right) \end{cases} \tag{12}$$

The equation used for controlling the bi-directional converter is as follows:

$$V_{SC} = L_{SC}i_{L_{SC}}(s)s + R_{Load}\, i_{L_{SC}}(s) + (1 - D_{SC}(s))V_{DC} \tag{13}$$

As a result, the following equation is established to connect the duty cycle DSC with the present ISC:

$$\frac{I_{SC}(s)}{D_{SC}(s)} = \frac{\frac{V_{DC}}{R_{Load}}}{1 + \frac{L_{SC}}{R_{Load}}s} \tag{14}$$

The compensator of transfer function is as described below:

$$G_{SC}(s) = \frac{K_{i_{SC}}\left(1 + \frac{K_{P_{SC}}}{K_{i_{SC}}}s\right)}{s} \tag{15}$$

The system's transfer function is made simpler by assuming a pole/zero and applying compensation: $\frac{K_{P_{SC}}}{K_{i_{SC}}} = \frac{L_{SC}}{R_{\mathrm{Load}}}$. The newly developed closed-loop transfer function has become;

$$CLTF_{SC}\ (s) = \frac{1}{1+\frac{R_{Load}}{V_{dc}K_{i_{SC}}}s}\ ,\ \tau_{SC} = \frac{R_{Load}}{V_{DC}K_{i_{SC}}} \tag{16}$$

Then,

$$K_{p_{SC}} = \frac{L_{SC}}{\tau_{SC} V_{DC}} \; , \; K_{i_{SC}} = \frac{R_{Load}}{\tau_{SC} V_{DC}} \tag{17}$$

In the same method for battery, we obtain;

$$CLTF_{batt}\,(s) = \frac{1}{1 + \frac{R_{Load}}{V_{DC} K_{i_{batt}}} s} \tag{18}$$

where, $\tau_{batt} = \frac{R_{Load}}{V_{DC} K_{batt}}$ then,

$$K_{p_{batt}} = \frac{L_{batt}}{\tau_{batt} V_{DC}} \; and, \; K_{i_{batt}} = \frac{R_{Load}}{\tau_{DC} V_{DC}} \; . \tag{19}$$

4. RESULTS AND DISCUSSION

4.1. Short-Time Experimental Evaluation

To rigorously evaluate the effectiveness of the proposed (EMS), a series of simulations were conducted using MATLAB-Simulink platforms. Four distinct simulation scenarios were developed, each employing different values of τ. The values chosen for τ were 0.1s, 0.5s, 1s, and 4s. These τ were crucial in determining how the system would respond to fluctuations in both power demand and energy supply. The simulations were initiated under specific conditions to ensure consistency and reliability in the results:

The solar power input varied throughout the simulations, with values fluctuating between 420 W/m^2 and 765 W/m^2. This range was selected to mimic real-world conditions where solar energy production can change due to factors such as weather or time of day. The electric demand was also variable, with set points of 600 W, 400 W, and 200 W. These fluctuations represent typical power requirements in HESS, addressing both peak and lower demand scenarios. The batteries commenced with a SOC of 50%, indicating that they were half-full at the beginning of the simulation. In contrast, the SC began with a SOC of 65.95%, reflecting their greater initial energy reserve.

Figs. 8-11 display the power waveforms for τ= 0.1s, 0.5s, 1s, and 4s, respectively. These figures collectively demonstrate how varying the LPF τ influences the performance of both the batteries and SC. The findings reveal that, when τ is set to a lower value (e.g., 0.1 s), the battery exhibits a sluggish response to power demands. This is primarily because the SC is actively managing peak power demands, allowing the battery to react more slowly. However, as τ increases, the SC takes on a greater role, leading to a reduction in the relative performance of the battery in terms of power delivery. Figs. 12-13 are shown the battery and SC current, respectively. A longer τ may assist in reducing the stress on the battery produced by abrupt variations in the load current. As a consequence, reaction times to rapid changes in load are also slower. In contrast, small τ, fast response by the battery resulting increase battery stress and minimize the lifespan of battery. Just the peak current is eliminated by the SCs. Nevertheless, when the T_c increases, the SCs are able to get rid of the peak current and guarantee an extended charging and discharging current.

Fig. 14 provides a comparative analysis of the SOC for the batteries across different when τ values. An increase in τ correlates with a decrease in the charge/discharge rate for the batteries (SOC_{bat}). This trend indicates that longer τ result in slower energy transfer rates for the batteries. Conversely, the (SOC_{SC})

show an increase in their charge/discharge rate with higher τ values, as shown in Fig. 15. This suggests that the SC are more effectively managing energy fluctuations when given more time to respond, thereby enhancing their ability to deliver energy during peak demand periods. The stability of the DC link voltage is illustrated in Fig. 16. Throughout the simulation, the DC link voltage maintained a consistent level of 100 V. This stability is crucial for ensuring that the energy management system operates effectively, as significant voltage fluctuations can lead to inefficiencies or system failures. The system achieved this reference voltage within a rapid timeframe of less than 0.05 s, with a minimal overshoot of less than 1%. This rapid stabilization underscores the effectiveness of the EMS in maintaining voltage levels despite the dynamic nature of solar irradiation and load demand. Furthermore, Fig. 17 illustrates the power balance at the DC link, which exhibits minimal variation, with a maximum peak of 200 W and fluctuations maintained within ±10 W. This stability in power balance is indicative of the EMS's effectiveness in managing energy distribution and consumption across the system.

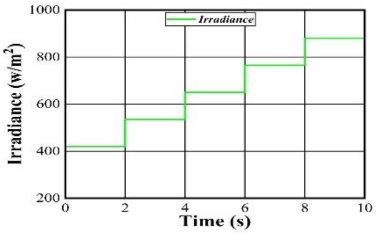

Fig. 7. Irradiation

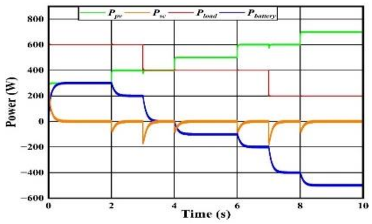

Fig. 8. Power waveforms with τ =0.1s.

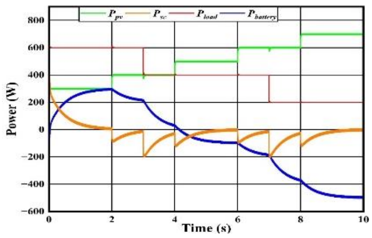

Figure 9. Power waveforms with τ =0.5 s

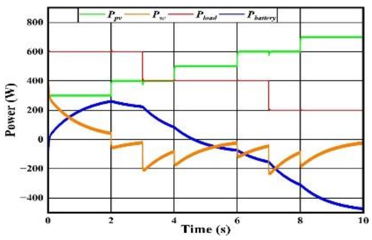

Figure 10. Power waveforms with τ =1 s

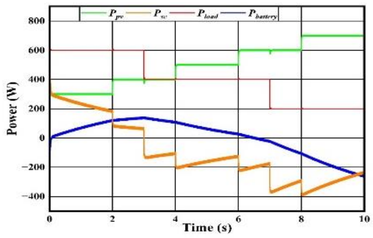

Figure 11. Power waveforms with τ = 4 s

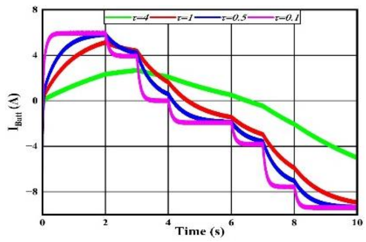

Figure 12. Current of battery

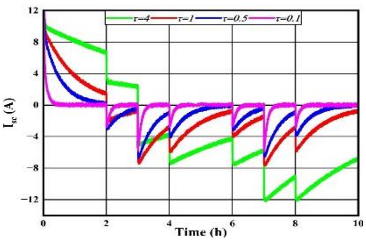

Figure 13. Current of SC

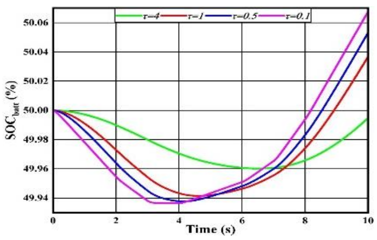

Figure 14. State of charge of battery

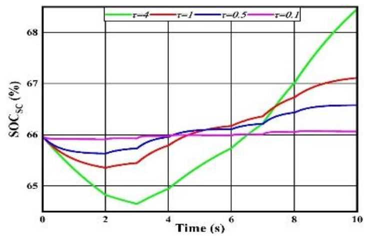

Figure 15. State of charge of SC

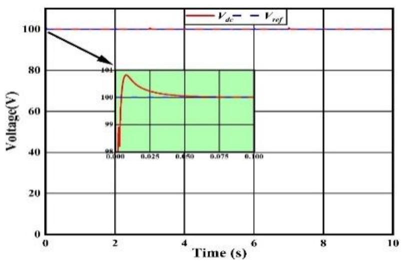

Figure 16. DC link voltage

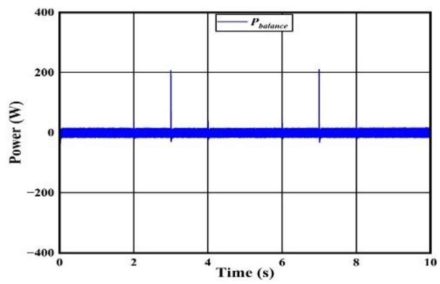

Figure 17. Power balance

4.2. One-Day Experimental Evaluation

This sub-section presents a comprehensive evaluation of the EMT using the same τ mentioned in the first scenario, based on a one-day dataset collected from a site in northern Algeria. The primary objective of this analysis is to examine the impact of varying τ on the energy consumption of HESS.

Fig. 18 illustrates the solar irradiance throughout the experimental period, providing crucial context for the subsequent EMT analysis. This variability in solar irradiance is a significant factor influencing the performance of the HESS. Figs. 19-22 depict the power profiles of the PV, battery, SC, and load for τ= 0.1s, 0.5s, 1s, and 4s, respectively. With τ set to a small value, it is evident that the SC primarily manages significant fluctuations in load. This rapid response capability enables the SC to effectively address immediate power demands, while the battery reacts to oscillations induced by changes in wind speed. The short τ allows for agile energy management, but it also results in limited energy storage capacity by the SC, as it is primarily focused on quick responses to load variations. Conversely, when τ is increased, the SC operates over a longer duration. This extended operational timeframe allows the SC to respond not only to load fluctuations but also to variations in wind energy. As a result, the SC alleviates the burden on the battery, enabling it to manage energy storage more efficiently. This transition signifies a shift in the EMT dynamics within the HESS, with the SC playing a more central role in energy balancing.

The current profiles of both the battery and SC are further explored in Figs. 23 and 24. The data indicates that a lower τ results in reduced energy storage and delivery capabilities by the SC. This is indicative of the SC's focus on immediate load support rather than long-term energy management. In contrast, a higher τ enhances the SC's ability to manage energy effectively, allowing for more substantial energy storage and delivery capabilities. Notably, the battery exhibits the opposite behavior, with increased τ leading to slower response rates and diminished power delivery efficiency.

Figs. 25 and 26 illustrate the state of charge (SOC) for both the battery and SC under all different τ. The data reveals that the SOC of the battery decreases at a slower rate when τ is higher, indicating a more conservative discharge profile. On the other hand, the SOC of the SC demonstrates increased variability with a higher τ, reflecting its enhanced role in managing energy fluctuations over longer periods.

Fig. 27 presents the DC bus voltage stability, which maintains a consistent level of 100 V throughout the simulation, despite rapid fluctuations in solar irradiance and load demand. The observed voltage ripple is approximately ±1%, signifying effective voltage regulation within the HESS. Such stability is paramount for the reliable operation of the EMT, as significant voltage fluctuations can adversely affect system performance.

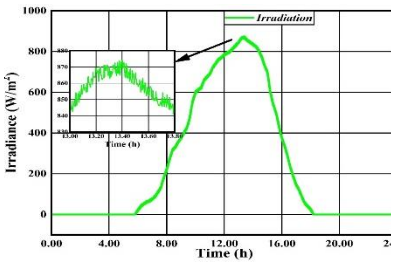

Figure 18. Irradiation

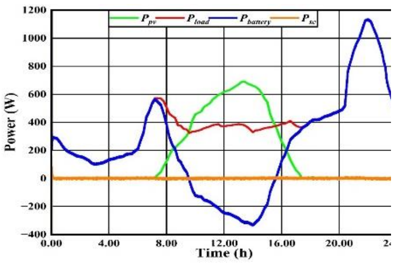

Figure 19. Power waveforms with τ =0.1 s

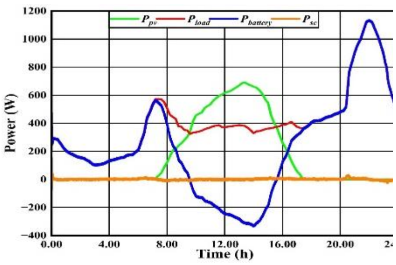

Figure 20. Power waveforms with τ =0.5 s

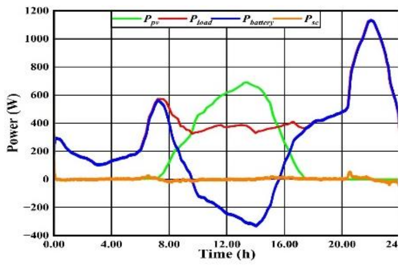

Figure 21. Power waveforms with τ =1 s

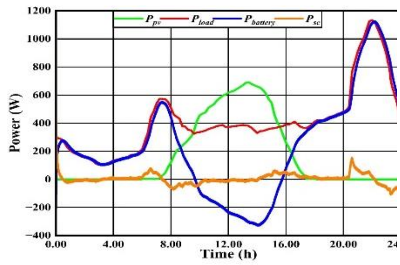

Figure 22. Power waveforms with τ = 4 s

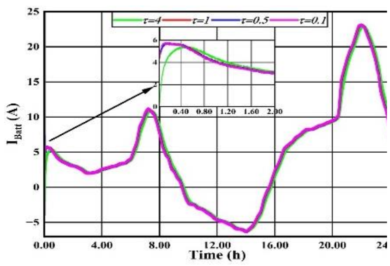

Figure 23. Current of battery

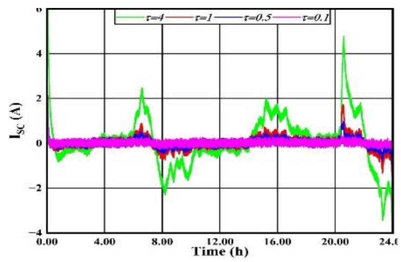

Figure 24. Current of SC

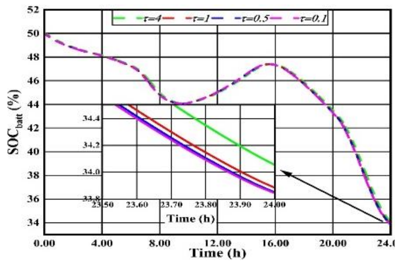

Figure 25. State of charge of battery

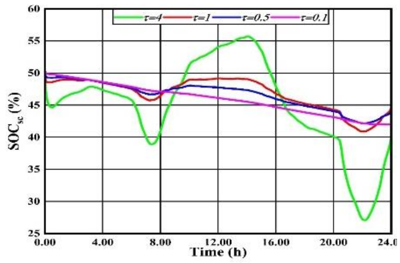

Figure 26. State of charge of SC

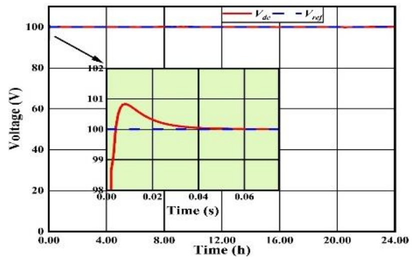

Figure 27. DC link voltage

5. CONCLUSIONS

This study introduces an innovative EMT for HESS in PV-powered applications. The suggested method utilizes LPF to improve power distribution between batteries and SCs, therefore improving system stability and prolonging battery lifespan. This work presents key innovations and contributions, including a novel LPF-based EMT for optimal power allocation, improved system stability via effective filtering of high-frequency power fluctuations, prolonged battery lifespan through minimized stress and optimized charge-discharge cycles, a comprehensive system model for precise simulation and analysis, and rigorous experimental validation showcasing the efficacy of the proposed method. The suggested energy management technique has substantial benefits compared to traditional methods, such as increased system efficiency, decreased operating costs, and better system dependability. The LPF-based solution may reduce the effects of intermittent renewable energy sources by efficiently controlling power flow between energy storage devices, hence ensuring a consistent and dependable power supply in distant regions. Future study may include investigating sophisticated control methodologies, like model predictive control and artificial intelligence, to enhance the efficacy of the energy management system. Furthermore, examining the effects of various LPF designs and temporal constants on system performance may provide significant insights for practical application. By focusing on these aspects, the suggested energy management method may be enhanced and used to a broader spectrum of applications. This approach improves energy stability and mitigates battery deterioration by effectively regulating power fluctuations. Comprehensive simulations validate the system's efficacy, demonstrating measurable improvements in battery state of charge and decreased stress levels. These results underscore the approach's capacity to markedly enhance the stability and longevity of energy systems in distant regions, representing progress in sustainable energy technology.

REFERENCES

[1] Bharatee A, Ray PK, Ghosh A. A Power Management Scheme for Grid-connected PV Integrated with Hybrid Energy Storage System. *J Mod Power Syst Clean Energy*. 2022 Jul;10(4):954-63. doi: 10.35833/MPCE.2021.000023.

[2] Rezk H, Nassef AM, Abdelkareem MA, Alami AH, Fathy A. Comparison among various energy management strategies for reducing hydrogen consumption in a hybrid fuel cell/supercapacitor/battery system. *Int J Hydrogen Energy*. 2021 Jan;46(8):6110-26. doi: 10.1016/j.ijhydene.2019.11.195.

[3] Jing W, Lai CH, Wong WSH, Wong MLD. A comprehensive study of battery-supercapacitor hybrid energy storage system for standalone PV power system in rural electrification. *Appl Energy*. 2018 Aug;224:340-56. doi: 10.1016/j.apenergy.2018.04.106.

[4] Cabrane Z, Ouassaid M, Maaroufi M. Management and control of storage photovoltaic energy using battery-supercapacitor combination. In: *2014 Second World Conference on Complex Systems (WCCS)*; 2014 Nov. p. 380-5. doi: 10.1109/ICoCS.2014.7060896.

[5] Lahyani A, Venet P, Guermazi A, Troudi A. Battery/Supercapacitors Combination in Uninterruptible Power Supply (UPS). *IEEE Trans Power Electron*. 2013 Apr;28(4):1509-22. doi: 10.1109/TPEL.2012.2210735.

[6] Adhikari S, Lei Z, Peng W, Tang Y. A battery/supercapacitor hybrid energy storage system for DC microgrids. In: *2016 IEEE 8th International Power Electronics and Motion Control Conference (IPEMC-ECCE Asia)*; 2016 May; Hefei, China. IEEE; 2016. p. 1747-53. doi: 10.1109/IPEMC.2016.7512558.

[7] Wen S, Wang S, Liu G, Liu R. Energy Management and Coordinated Control Strategy of PV/HESS AC Microgrid During Islanded Operation. *IEEE Access*. 2019;7:4432-41. doi: 10.1109/ACCESS.2018.2887114.

[8] Abishek M, Gokul R, Karthiga P, Lokesh P, Banumathi S. Power Management For Pv-Wind And Hybrid Energy Storage Integrated Micro Grid. In: *2023 9th International Conference on Electrical Energy Systems (ICEES)*; 2023 Mar. p. 334-40. doi: 10.1109/ICEES57979.2023.10110096.

[9] Altin N, Eyimaya SE. A Combined Energy Management Algorithm for Wind Turbine/Battery Hybrid System. *J Electron Mater*. 2018 Aug;47(8):4430-6. doi: 10.1007/s11664-018-6159-z.

[10] ElGhanam E, Sharf H, Hassan MS, Osman A. Performance Evaluation of Hybrid Battery–Supercapacitor-Based Energy Storage Systems for Urban-Driven Electric Vehicles. *Sustainability*. 2023 Jan;15(11):8747. doi: 10.3390/su15118747.

[11] Serban I, Marinescu C. Battery energy storage system for frequency support in microgrids and with enhanced control features for uninterruptible supply of local loads. *Int J Electr Power Energy Syst*. 2014 Jan;54:432-41. doi: 10.1016/j.ijepes.2013.07.004.

[12] Albasheri MA, Bouchhida O, Soufi Y, Cherifi A. Enhanced supervisor energy management technique of DC microgrid-based PV/wind/battery/SC. *Electr Eng*. 2024 Aug. doi: 10.1007/s00202-024-02622-2.

[13] Abdulelah AM, Ouahid B, Youcef S. Control of a Stand-Alone Variable Speed Wind Turbine with a Permanent Magnet Synchronous Generator. In: *2021 18th International Multi-Conference on Systems, Signals Devices (SSD)*; 2021 Mar. p. 546-50. doi: 10.1109/SSD52085.2021.9429307.

[14] Wang Y, Wang L, Li M, Chen Z. A review of key issues for control and management in battery and ultra-capacitor hybrid energy storage systems. *eTransportation*. 2020 May;4:100064. doi: 10.1016/j.etran.2020.100064.

[15] Babu TS, Vasudevan KR, Ramachandaramurthy VK, Sani SB, Chemud S, Lajim RM. A Comprehensive Review of Hybrid Energy Storage Systems: Converter Topologies, Control Strategies and Future Prospects. *IEEE Access*. 2020;8:148702-21. doi: 10.1109/ACCESS.2020.3015919.

[16] Albasheri MA, Bouchhida O, Soufi Y, Cherifi A. Enhanced energy storage system efficiency for remote area-based DC microgrid. *Stud Eng Exact Sci*. 2024 Jul;5(2):e5367. doi: 10.54021/seesv5n2-002.

[17] Mesbahi T, Rizoug N, Bartholomeüs P, Sadoun R, Khenfri F, Le Moigne P. Optimal Energy Management for a Li-Ion Battery/Supercapacitor Hybrid Energy Storage System Based on a Particle Swarm Optimization Incorporating Nelder–Mead Simplex Approach. *IEEE Trans Intell Veh*. 2017 Jun;2(2):99-110. doi: 10.1109/TIV.2017.2720464.

[18] Albasheri MA, Bouchhida O, Soufi Y, Cherifi A. Energy Management of Wind Energy Hybrid Storage for Remote Area Power System. In: *2024 12th International Conference on Smart Grid (icSmartGrid)*; 2024 May. p. 418-22. doi: 10.1109/icSmartGrid61824.2024.10578267.

[19] Zemirline N, Kabeche N, Moulahoum S. Artificial neural network controller for grid current quality improvement in solid-state transformers. *J Power Electron*. 2024 May;24(5):799-809. doi: 10.1007/s43236-023-00761-6.

[20] Cook MD, Parker GG, Robinett RD, Weaver WW. Decentralized Mode-Adaptive Guidance and Control for DC Microgrid. *IEEE Trans Power Deliv*. 2017 Feb;32(1):263-71. doi: 10.1109/TPWRD.2016.2583384.

[21] Hartani MA, Hamouda M, Abdelkhalek O, Mekhilef S. Sustainable energy assessment of multi-type energy storage system in direct-current-microgrids adopting Mamdani with Sugeno fuzzy logic-based energy management strategy. *J Energy Storage*. 2022 Dec;56:106037. doi: 10.1016/j.est.2022.106037.

[22] Yi Z, Dong W, Etemadi AH. A Unified Control and Power Management Scheme for PV-Battery-Based Hybrid Microgrids for Both Grid-Connected and Islanded Modes. *IEEE Trans Smart Grid*. 2018 Nov;9(6):5975-85. doi: 10.1109/TSG.2017.2700332.

[23] Albasheri MA, Bouchhida O, Soufi Y, Cherifi A. Enhanced Vector Control of Induction Motor by Fuzzy Logic Controller. In: *2024 2nd International Conference on Electrical Engineering and Automatic Control (ICEEAC)*; 2024 May. p. 1-5. doi: 10.1109/ICEEAC61226.2024.10576217.

[24] Qi W, Li Y, Li H, Wayne SW, Lin X. The development and numerical verification of a compromised real time optimal control algorithm for hybrid electric vehicle. *J Power Sources*. 2019 Dec;443:227272. doi: 10.1016/j.jpowsour.2019.227272.

[25] Ghadbane HE, Barkat S, Houari A, Djerioui A, Abdelhak H, Mesbahi T. A Load Following Energy Management Strategy for a Battery-Supercapacitor Hybrid Power System Implemented with a PIL Co-Simulation Approach. *Smart Grids Energy*. 2024 Jul;9(2):32. doi: 10.1007/s40866-024-00214-4.

[26] Dao HV, et al. Optimization-Based Fuzzy Energy Management Strategy for PEM Fuel Cell/Battery/Supercapacitor Hybrid Construction Excavator. *Int J Precis Eng Manuf Green Tech*. 2021 Jul;8(4):1267-85. doi: 10.1007/s40684-020-00262-y.

[27] Zemirline N, Kabeche N, Moulahoum S. Grid current quality improvement for solid state transformer with an improved current controller. *Electr Power Syst Res*. 2024 Nov;236:110921. doi: 10.1016/j.epsr.2024.110921.

[28] Ma Z, et al. Optimal SOC Control and Rule-Based Energy Management Strategy for Fuel-Cell-Based Hybrid Vessel including Batteries and Supercapacitors. *J Mar Sci Eng*. 2023 Feb;11(2):398. doi: 10.3390/jmse11020398.

[29] Atif. Fuzzy logic controller for solar power smoothing based on controlled battery energy storage and varying low pass filter. *IET Renew Power Gener*. 2020. doi: 10.1049/iet-rpg.2020.0459.

[30] Ramos GA, Costa-Castelló R. Energy Management Strategies for Hybrid Energy Storage Systems Based on Filter Control: Analysis and Comparison. *Electronics*. 2022 Jan;11(10):1631. doi: 10.3390/electronics11101631.

[31] Cabrane Z, Ouassaid M, Maaroufi M. Analysis and evaluation of battery-supercapacitor hybrid energy storage system for photovoltaic installation. *Int J Hydrogen Energy*. 2016 Dec;41(45):20897-907. doi: 10.1016/j.ijhydene.2016.06.141.

[32] Cabrane Z, Kim J, Yoo K, Ouassaid M. HESS-based photovoltaic/batteries/supercapacitors: Energy management strategy and DC bus voltage stabilization. *Sol Energy*. 2021 Mar;216:551-63. doi: 10.1016/j.solener.2021.01.048.

[33] Li H, Kang J, Li C. Energy Management Strategy Based on Reinforcement Learning and Frequency Decoupling for Fuel Cell Hybrid Powertrain. *Energies*. 2024 Jan;17(8):1929. doi: 10.3390/en17081929.

[34] Tao F, Zhu L, Fu Z, Si P, Sun L. Frequency Decoupling-Based Energy Management Strategy for Fuel Cell/Battery/Ultracapacitor Hybrid Vehicle Using Fuzzy Control Method. *IEEE Access*. 2020;8:166491-502. doi: 10.1109/ACCESS.2020.3023470.

[35] Worku MY, Hassan MA, Abido MA. Real Time-Based under Frequency Control and Energy Management of Microgrids. *Electronics*. 2020 Sep;9(9):1487. doi: 10.3390/electronics9091487.

[36] Mujammal MAH, Moualdia A, Boulkhrachef S, Wira P, Boudana D, Albasheri MA. Advancing wind energy conversion: smart maximum power point based on M5-Pruned algorithm for enhanced wind energy production. *Prod Eng Res Devel*. 2024 Oct. doi: 10.1007/s11740-024-01315-w.

[37] Mujammal MAH, Moualdia A, Boulkhrachef S, Boudana D, Wira P, Albasheri MA. Next-Generation MPPT: neural network-driven optimization for superior solar performance. *Stud Eng Exact Sci*. 2024 Sep;5(2):e7338. doi: 10.54021/seesv5n2-150.

[38] Mujammal MAH, Moualdia A, Bouchhida O, Albasheri MA. Upgrade Perturbation and Observation of MPPT Strategy via Fuzzy Logic Controller. In: *2023 2nd International Conference on Electronics, Energy and Measurement (IC2EM)*; 2023 Nov. p. 1-7. doi: 10.1109/IC2EM59347.2023.10419670.

[39] Albasheri MA, Bouchhida O, Soufi Y, Moualdia A, Mujammal M. Control and Power Management of DC Microgrid Based Wind/Battery/Supercapacitor. In: *2022 IEEE 2nd International Maghreb Meeting of the Conference on Sciences and Techniques of Automatic Control and Computer Engineering (MI-STA)*; 2022 May. p. 680-5. doi: 10.1109/MI-STA54861.2022.9837665.

[40] Truong HVA, et al. Mapping Fuzzy Energy Management Strategy for PEM Fuel Cell–Battery–Supercapacitor Hybrid Excavator. *Energies*. 2020 Jan;13(13):3387. doi: 10.3390/en13133387.

[41] Abdulelah AM, Ouahid B, Youcef S, Abderrezzak C, Abdelhafidh M, Ahmed M. Improve Lifespan of Battery Energy Storage in Remote Area Power System. In: *2023 2nd International Conference on Electronics, Energy and Measurement (IC2EM)*; 2023 Nov. p. 1-6. doi: 10.1109/IC2EM59347.2023.10419419.

[42] Cau G, Cocco D, Petrollese M, Kær SK, Milan C. Energy management strategy based on short-term generation scheduling for a renewable microgrid using a hydrogen storage system. *Energy Convers Manag*. 2014 Nov;87:820-31. doi: 10.1016/j.enconman.2014.07.078.

[43] R. S, Kowsalya M. HESS-based microgrid control techniques empowered by artificial intelligence: A systematic review of grid-connected and standalone systems. *J Energy Storage*. 2024 Apr;84:111012. doi: 10.1016/j.est.2024.111012.

[44] Ali M, Hossain MI, Shafiullah M. Fuzzy Logic for Energy Management in Hybrid Energy Storage Systems Integrated DC Microgrid. In: *2022 International Conference on Power Energy Systems and Applications (ICoPESA)*; 2022 Feb. p. 424-9. doi: 10.1109/ICoPESA54515.2022.9754406.

[45] Ma T, Yang H, Lu L. Development of hybrid battery–supercapacitor energy storage for remote area renewable energy systems. *Appl Energy*. 2015 Sep;153:56-62. doi: 10.1016/j.apenergy.2014.12.008.
[46] Nambisan P, Khanra M. Optimal Energy Management of Battery Supercapacitor Aided Solar PV Powered Agricultural Feed Mill Using Pontryagin's Minimum Principle. *IEEE Trans Power Electron*. 2022 Feb;37(2):2216-25. doi: 10.1109/TPEL.2021.3104347.
[47] Zhang R, Hredzak B, Morstyn T. Distributed Control with Virtual Capacitance for the Voltage Restorations, State of Charge Balancing, and Load Allocations of Heterogeneous Energy Storages in a DC Datacenter Microgrid. *IEEE Trans Energy Convers*. 2019 Sep;34(3):1296-308. doi: 10.1109/TEC.2018.2889065.
[48] R. S, Kowsalya M. HESS-based microgrid control techniques empowered by artificial intelligence: A systematic review of grid-connected and standalone systems. *J Energy Storage*. 2024 Apr;84:111012. doi: 10.1016/j.est.2024.111012.
[49] Albasheri MA, Soufi Y, Bouchhida O, Cherifi A. Control and Energy Management Based on Decoupling Frequency of DC Microgrid. In: *2024 21st International Multi-Conference on Systems, Signals & Devices (SSD)*; 2024 Apr. p. 224-9. doi: 10.1109/SSD61670.2024.10549218.
[50] Mujammal MAH, Moualdia A, Wira P, Albasheri MA, Cherifi A. Novel Direct Power Control Based on Grid Voltage Modulated Strategy Using Artificial Intelligence. *Smart Grids Energy*. 2024 Oct;9(2):37. doi: 10.1007/s40866-024-00225-1.
[51] Benyoucef K, Moualdia A, Boudana D, Mujammal MAH, Albasheri MA. Optimal control strategies for DFIG-based wind turbines: simulation and analysis. *Stud Eng Exact Sci*. 2024 Dec;5(3):e12580. doi: 10.54021/seesv5n3-042.